Medical Journal of Bakırköy

Med J Bakirkoy 2023;19:256-262
DOI: 10.4274/BMJ.galenos.2023.2023.3-19

Research

Differentiating Renal Cell Carcinoma and Minimal Fat Angiomyolipoma with Volumetric MRI Histogram Analysis

Renal Hücreli Karsinom ve Minimal Yağ Anjiyomiyolipomunun Volümetrik MRG Histogram Analizi ile Ayrımı

Özlem Akıncı, Furkan Türkoğlu, Mustafa Orhan Nalbant, Ercan İnci

University of Health Sciences Türkiye, Bakırköy Dr. Sadi Konuk Training and Research Hospital, Clinic of Radiology, İstanbul, Türkiye

ABSTRACT

Objective: In this study, the utility of histogram parameters derived from diffusion-weighted imaging to differentiate renal cell carcinoma (RCC) from renal minimal fat angiomyolipoma (MFAML) was investigated.

Methods: In this retrospective study, 98 patients who were histopathologically diagnosed with RCC and MFAML and who underwent magnetic resonance imaging (MRI) examinations between 2015 and 2022 were included. Demographic data, preoperative MRI findings, MRI apparent diffusion coefficient (ADC) histogram analyses, operation types, and postoperative histopathological data of the patients were recorded. The mean, minimum (min), maximum (max), 5th, 10th, 25th, 50th, 75th, 90th, and 95th percentiles as well as skewness, kurtosis, and variance of ADC values were calculated.

Results: The study included 61 males and 37 females. Eighty eight of the patients had RCC and 10 had AML. In terms of age and gender, there was no significant difference between the two groups. The AML group's ADCmin, ADCmedian, ADCmean, ADCmax, 5th, 10th, 25th, 50th, 75th, 90th, and 95th percentiles were all lower than those of the RCC group. ADCmax value ($p<0.001$), as well as ADCmedian and the 50th, 75th, 90th, and 95th percentiles of ADC values ($p<0.05$), demonstrated a statistically significant difference. However, there was no statistical significance between ADCmin, ADCmean, and the 5th, 10th, and 25th percentiles of ADC values ($p>0.05$). The area under the curve, sensitivity, and specificity of the ADCmax value were 0.795, 62.4%, and 88.9%, respectively.

Conclusion: A whole tumor histogram and textural analysis of ADC values could be useful in distinguishing MFAML from RCC.

Keywords: Renal cell carcinoma, renal angiomyolipoma, magnetic resonance imaging, diffusion weighted imaging, histogram analysis

ÖZ

Amaç: Bu çalışmada, difüzyon ağırlıklı görüntülemeden elde edilen histogram parametrelerinin, renal hücreli karsinomu (RHK) renal minimal yağ anjiyomiyolipomdan (MYAML) ayırt etmede etkinliği araştırıldı.

Gereç ve Yöntem: Bu retrospektif çalışmaya histopatolojik olarak RHK ve MYAML tanısı alan ve 2015 ve 2022 yılları arasında manyetik rezonans görüntülemesi (MRG) yapılan 98 hasta dahil edildi. Hastaların demografik verileri, preoperatif MRG bulguları, MRG görünür difüzyon katsayısı (ADC) histogram analizleri, operasyon tipleri, postoperatif histopatolojik verileri kaydedildi. Ortalama, minimum (min), maksimum (maks), medyan 5., 10., 25., 50., 75., 90. ve 95. yüzdelikleri içeren ADC değerlerinin histogram parametreleri ile çarpıklık, basıklık ve varyansı hesaplandı.

Bulgular: Çalışmaya 61 erkek ve 37 kadın dahil edildi. Hastaların 88'i RHK idi ve 10'u MYAML idi. İki grup arasında yaş ve cinsiyet açısından anlamlı fark yoktu. MYAML grubunun ADCmin, ADCmedyan, ADCortalama, ADCmaks, 5., 10., 25., 50., 75., 90. ve 95. yüzdeliklerinin tümü RHK grubundan düşüktü. ADCmaks değeri ($p<0,001$) ile ADCmedyan ve ADC değerlerinin 50., 75., 90. ve 95. yüzdelikleri ($p<0,05$) istatistiksel olarak anlamlı fark gösterdi. Bununla birlikte, ADCmin, ADCortalama ve ADC değerlerinin 5., 10. ve 25. yüzdelikleri arasında istatistiksel anlamlı fark yoktu ($p>0,05$). ADCmaks değerinin eğri altındaki alanı, duyarlılık ve özgüllüğü sırasıyla 0,795, %62,4 ve %88,9 idi.

Sonuç: Tüm tümör histogramı ve ADC değerlerinin doku analizi, MYAML'yi RHK'den ayırt etmede yararlı olabilir.

Anahtar Kelimeler: Renal hücreli karsinom, renal anjiyomiyolipom, manyetik rezonans görüntüleme, difüzyon ağırlıklı görüntüleme, histogram analizi

Address for Correspondence: Özlem Akıncı, University of Health Sciences Türkiye, Bakırköy Dr. Sadi Konuk Training and Research Hospital, Clinic of Radiology, İstanbul, Türkiye
Phone: +90 505 628 25 28 E-mail: dr.ozlemgungor@yahoo.com ORCID ID: orcid.org/0000-0002-6615-4892

Cite as: Akıncı Ö, Türkoğlu F, Nalbant MO, İnci E. Differentiating Renal Cell Carcinoma and Minimal Fat Angiomyolipoma with Volumetric MRI Histogram Analysis. Med J Bakirkoy 2023;19:256-262

Received: 11.04.2023
Accepted: 04.06.2023

INTRODUCTION

Renal angiomyolipoma (AML) is a benign kidney tumor that can contain a variety of cell types, including blood vessels, smooth muscle cells, and adipose tissue (1). Because of their macroscopic fat, most AML can be easily identified on computed tomography or magnetic resonance imaging (MRI), but only around 5% of AML can be observed on imaging without any visible fat [minimal fat AML (MFAML)] (2,3). It is vital to differentiate AML from renal cell carcinoma (RCC) because AML, particularly when it is tiny and asymptomatic, can be monitored without any therapy, but RCC often requires surgical excision (4). Despite different MRI characteristics, MFAML may be difficult to distinguish from other renal malignant tumors, particularly clear cell renal cell carcinoma (ccRCC), which accounts for 75% of all RCCs in adults (5). Diffusion-weighted imaging (DWI) has been shown to be beneficial for the functional assessment of renal malignancies. This makes it possible to characterize tumors in a noninvasive manner (6-8).

DWI apparent diffusion coefficient (ADC) can indicate tissue water molecular diffusion and distinguish benign from malignant kidney lesions. Most earlier research evaluated ADC values using manually defined regions of interest (ROIs) on the tumor's largest practical section, which did not accurately reflect its diffusion characteristics (9,10).

The volumetric ADC histogram of the entire lesion was used to assess ADC values across the lesion without ROI placement to ensure repeatability and calculation accuracy. Histogram analysis is a statistical tool for assessing the properties of all vowels in an ROI to better estimate the tumor biological characteristics and histological heterogeneity (11). By recording the ADC values throughout the whole tumor, this technique can remove sampling bias.

The utility of DWI histogram analysis in the differential diagnosis of RCC and MFAML has been investigated in a very limited amount of published studies. The aim of this study was to investigate the ability of the ADC histogram and textural analysis to distinguish between MFAML and RCC.

METHODS

This retrospective study included 98 patients who were diagnosed with RCC and AML during postoperative histopathological examination between January 2015 and December 2022 and who had pre-operative MRI images. An approval from an University of Health Sciences Türkiye, Bakırköy Dr. Sadi Konuk Training and Research Hospital Clinical Research Ethics Committee was obtained for the study (decision no: 2023-01-15, date: 09.01.2023). Patients who were histopathologically diagnosed with RCC and AML, did not receive radiotherapy or chemotherapy before surgery, did not contain macroscopic fat, and did not have motion artifacts that would impair image quality were included in the study.

Patients who had no preoperative MRI (n=10), had typical findings of AML on conventional MRI (n=8), were getting cancer treatment before an MRI exam (n=15), had imaging artifacts that make diagnosing lesions more difficult (n=10), had an interval between surgery and an MRI examination longer than one month (n=17), had a pathological diagnosis other than RCC or AML (n=8), or had undergone kidney surgery in the past for any reason (n=7) were excluded from the study. There were 75 patients excluded. Our study included 98 patients, 88 of whom had RCC and 10 of whom had AML. In the calculation made for the power analysis carried out with the G Power 3.1.9.7 (Franz Faul, Germany) program, it was assumed that the effect size would be d=1.205. In the calculation made with the determined effect size and a 5% margin of error, the strength of the study was found to be 86.9%.

Demographic data, preoperative MRI findings, MRI ADC histogram analyses, operation types, and postoperative histopathological data of the patients were recorded. Data from MRI ADC histograms were compared between the groups.

On a 3.0 T magnetic resonance system, a 16-channel phased array surface coil was used to receive the signal (Siemens Medical Solutions, Erlagen, Germany). DWI was administered at b-values of 1000 s/mm^2. The minimum (min) fasting time required before an MRI is four hours. Transverse, sagittal, and coronal thin-section turbo spin-echo T2-weighted images were acquired (20 slices; thickness: 3 mm with no intersection gap (IG); TR/TE: 5800/100 ms; number of signals acquired: 2; resolution: 0.8 mm 0.8 mm). The axial images at b values of 1000 s/mm^2 were acquired with respiratory-triggered single-shot echo-planar sequences [matrix, 160x192; field of view, 36-44 cm; slice thickness, 4 mm; IG, 1 mm; bandwidth (kHz/pixel), 250; acquisition time (ms) 4-5; flip angle (degrees) 90; number of excitations (NEX), 6].

Image Analysis

All of the raw data from the DWI was transferred to a personal computer using the picture archiving and communication system, where it was then processed using the voxel program LIFEx 7.2.0, (https://lifesoft.org) which is free and open source. All MR scans were independently

reviewed by two radiologists (8 years of experience each in abdominal MRI) who were blinded to the clinical data and histopathologic findings. The axial T2-weighted images were used as a guide to manually draw the ROI encompassing the lesion in each segment. Automatically, the data from each ROI was combined into a volumetric ROI that described the entire tumor in voxels (Figure 1, 2). The following model was then used to create a volumetric ADC map: Diffusion-induced signal attenuation is denoted by S = S0 exp(b ADC), where S0 is the signal intensity without diffusion sensitization and b is the value that sets the level of diffusion weighting in the signal. The min, maximum (max), skewness and variance of ADC values as well as the 5th, 10th, 25th, 50th, 75th, 90th, and 95th percentiles were determined. The point on the left where n% of the voxel values from that histogram were observed was the nth percentile. Positive skewness, which reflects the deviation of the distribution median from the mean value, indicates that the right tail

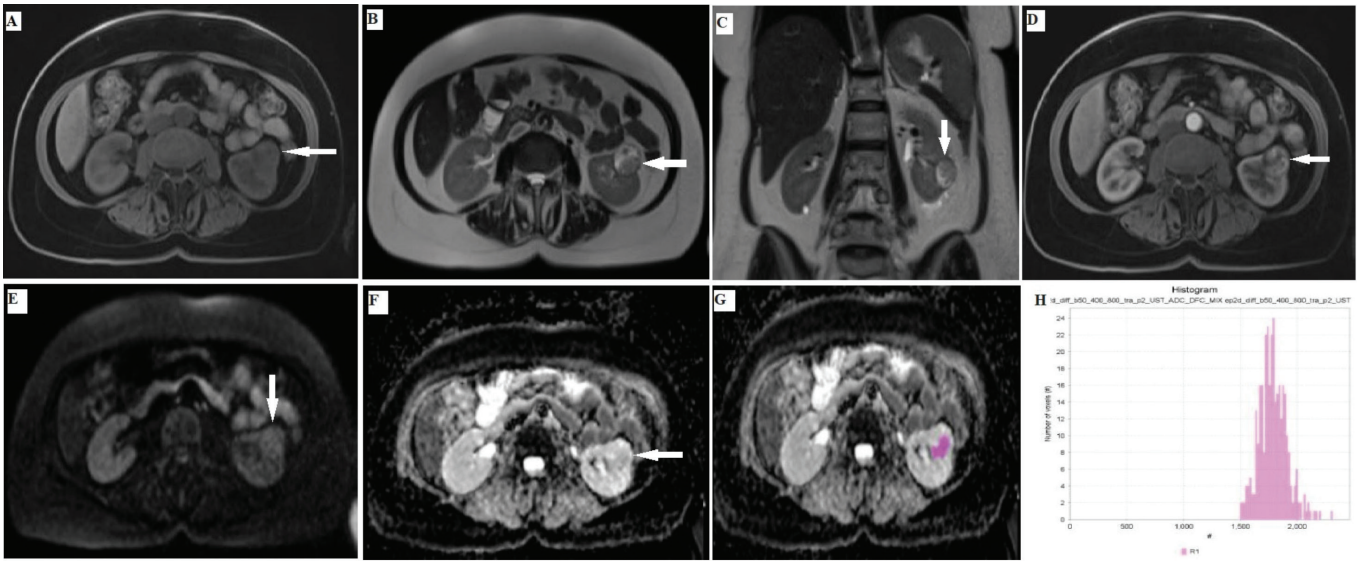

Figure 1. Clear cell renal cell carcinoma in a 65-year-old woman. (A) The axial T1-weighted fat suppression image of the lesion exhibits a low signal intensity; (B) On the axial T2-weighted image, the lesion has a high signal intensity; (C) On the coronal T2-weighted image, the lesion exhibits strong signal intensity; (D) On the axial T1-weighted post contrast fat supression image, the lesion exhibits strong contrast enhancement; (E) Diffusion-weighted imaging reveals concrete restricted diffusion around the lesion; (F) Lesion shows low apparent diffusion coefficient (ADC) on ADC; (G) Lesion color ADC map, freehand region of interest schematic; (H) ADC value was concentrated on the right side of the histogram, as shown by the corresponding volumetric histogram

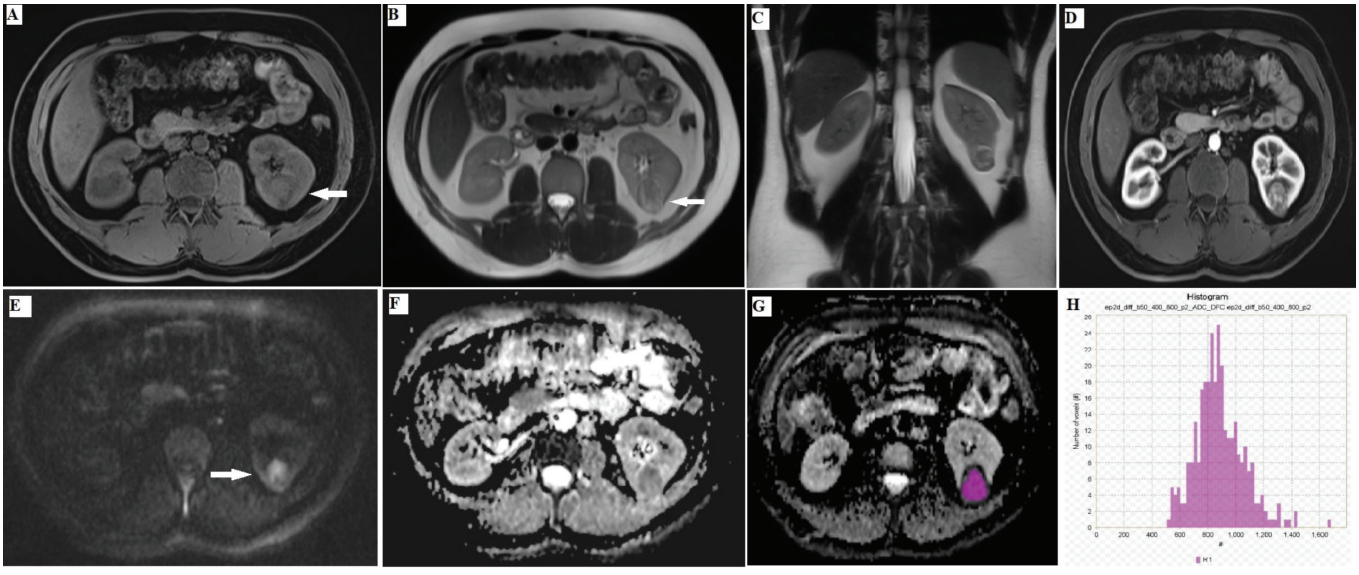

Figure 2. Angiomyolipoma of the kidney in a 55-year-old woman. (A) The axial T1-weighted fat suppression image of the lesion exhibits a low signal intensity; (B) On the axial T2-weighted image, the lesion has a high signal intensity; (C) On the coronal T2-weighted image, the lesion exhibits strong signal intensity; (D) On the axial T1-weighted post contrast fat supression image, the lesion exhibits a slight contrast enhancement; (E) Diffusion-weighted imaging reveals concrete restricted diffusion around the lesion; (F) Lesion displays low apparent diffusion coefficient (ADC); (G) Lesion color ADC map, freehand region of interest schematic, and diffusion image; (H) ADC value was concentrated on the middle and left of the volumetric histogram, according to the corresponding histogram

of the distribution is flatter or longer than the left tail. The peakiness of the histogram distribution is reflected by kurtosis. High kurtosis distributions have heavy tails, a sharp peak close to the mean, and a rapid decline.

Statistical Analysis

Statistical analysis was performed using IBM SPSS 23.0 (Chicago, IL, United States). Using the data set created by integrating the ADC measurements of each patient in the RCC and AML groups, histograms of the groups were generated. All patient measurements displayed a distributional variance, as indicated by the histograms. Using these measurements, descriptive statistics such as mean, min, median, max, standard deviation, skewness, kurtosis, and percentiles were computed for each patient group, and changes in these descriptive statistics were graphically displayed. The calculation of these group statistics relied on individuals. Using the t-test for independent samples, it was determined whether the statistics produced by individuals varied between groups. On the basis of individual data, receiver operating characteristic (ROC) curves were generated and a threshold value was determined for the compiled statistics. Sensitivity and specificity values were calculated for threshold values.

RESULTS

Demographic Data

In the study, 61 males and 37 females were included (Table 1). Eighty eight of the patients were RCC and 10 were MFAML. There was no significant difference between the two groups in terms of age and gender (respectively; p=0.099, and p=0.006).

Results of ADC Histogram Parameters

All of the ADC percentiles, including the min, median, mean, and max values, as well as the 5th, 10th, 25th, 50th, 75th, 90th, and 95th percentiles, were lower for the AML group than they were for the RCC group (Table 2). ADCmax value (p<0.001), as well as ADCmedian and the 50th, 75th, 90th,

Table 1. Demographic, radiological and pathological data of patients

	RCC n (%)/mean ± SD	MFAML n (%)/mean ± SD	p-value
Age	56.22±12.56	49.5±12.05	0.099[a]
Sex (male/female)	59 (67.0)/29 (33.0)	2 (20.0)/8 (80.0)	**0.006**[b]
Tumor diameter (mm)	54.89±32.92	47.3±41.92	0.228[a]

[a]Mann-Whitney U test, [b]Chi-square test. RCC: Renal cell carcinoma, MFAML: Minimal fat angiomyolipoma, SD: Standard deviation

Table 2. Comparisons of ADC histogram parameters between RCC and AML

ADC (10^{-3} mm^2/s)	RCC	AML	Total	p-value	Significance level
Mean	1.295±0.410	1.089±0.215	1.274±0.398	0.051	-
Standard deviation	0.246±0.133	0.162±0.083	0.238±0.131	**0.015**	95%
Median	1.303±0.427	1.081±0.218	1.281±0.416	**0.050**	95%
Minimum	0.609±0.482	0.751±0.260	0.624±0.465	0.196	-
Maximum	1.987±0.618	1.490±0.272	1.936±0.610	**0.003**	99%
Skewness	-0.1±0.6	0.3±0.3	0.0±0.6	**0.041**	95%
Kurtosis	0.7±1.5	-0.4±0.5	0.6±1.4	**0.007**	99%
5th	0.860±0.407	0.838±0.208	0.858±0.391	0.833	-
10th	0.985±0.388	0.879±0.2	0.974±0.374	0.291	-
25th	1.145±0.394	0.962±0.194	1.127±0.382	0.087	-
50th	1.303±0.427	1.081±0.218	1.281±0.416	**0.050**	95%
75th	1.450±0.447	1.207±0.248	1.425±0.436	**0.036**	95%
90th	1.597±0.480	1.321±0.285	1.569±0.471	**0.026**	95%
95th	1.685±0.504	1.354±0.309	1.653±0.497	**0.019**	95%

ADC: Apparent diffusion coefficient, RCC: Renal cell carcinoma, AML: Angiomyolipoma

and 95th percentiles of ADC values ($p<0.05$), demonstrated a statistically significant difference. However, there was no statistical significance between ADCmin, ADCmean, and the 5th, 10th, and 25th percentiles of ADC values ($p>0.05$). The RCC group had higher variance, skewness, and kurtosis than the AML group ($p<0.05$).

Diagnostic Performance

The ROC curve demonstrated the efficacy of ADC histogram parameters in the diagnosis of RCC; the ADCmax value had the highest area under the curve (AUC) (0.795), and the sensitivity and specificity under the threshold value of $1.794x10^{3}$ mm^2/s were 62.4% and 88.9%, respectively. The effectiveness of the diagnostic procedure was then followed by kurtosis. Under the threshold of 0.0, the sensitivity and specificity were respectively 61.2% and 77.8%. The AUC was greater than the value of the ADC at the 95th percentile of its distribution (0.738). Under the cut-off value of $1.594x10^{-3}$ mm^2/s, the sensitivity and specificity were 57.6% and 77.8%. The AUC was 0.727 which corresponded to the 90th percentile of the ADC value. Under the cut-off value of $1.611x10^{-3}$ mm^2/s, the sensitivity and specificity were 54.1% and 88.9% (Table 3).

The variance and the 75th percentile of the ADC value both contributed to a higher AUC (AUC =0.715). Under the threshold values of 0.181 and $1.445x10^{-3}$ mm^2/s, the sensitivity and specificity were 68.2% and 77.8% and 56.5% and 88.9%, respectively. The AUC was also higher with the ADCmedian and 50th percentile of the ADC value (AUC =0.708). With the cut-off value of $1.219x10^{-3}$ mm^2/s, the sensitivity and specificity were 58.8% and 77.8% for both parameters (Table 3).

DISCUSSION

Before surgical treatment, MFAML is frequently misdiagnosed as RCC (12). It is difficult but necessary for treatment planning and prognosis evaluation to distinguish between these two conditions (13). Histopathology is the gold standard in the differential diagnosis of MFAML and RCC. MFAML and RCC have similar imaging characteristics, which makes the differentiating diagnosis by traditional imaging modalities challenging (14). Most prior research used various DWI approaches to differentiate renal neoplasms due to the limited information identified by conventional MRI. According to a meta-analysis by Tordjman et al. (15), ADC of renal tumors that exclude cystic and necrotic areas has a greater ability to distinguish RCC from other renal lesions than whole-lesion ADC. According

Table 3. ROC results of ADC metrics histogram parameters

Test result variable(s)	AUC	Standard error[a]	Asymptotic sig.[b]	Asymptotic 95% confidence interval				
				Lower Bound	Upper Bound	Cut-off	Sensitivity	Specificity
Mean	0.708	0.062	0.040	0.586	0.831	1.267	0.565	0.889
Standard deviation	0.715	0.093	**0.035**	0.533	0.897	0.181	0.682	0.778
Median	0.708	0.063	**0.040**	0.585	0.832	1.219	0.588	0.778
Minimum	0.618	0.066	0.245	0.252	0.511	0.851	0.294	0.889
Maximum	0.795	0.058	**0.004**	0.681	0.908	1.794	0.624	0.889
Skewness	0.690	0.068	**0.062**	0.176	0.443	0.4	0.212	0.778
Kurtosis	0.748	0.073	**0.015**	0.606	0.891	0.0	0.612	0.778
5th	0.544	0.065	0.667	0.416	0.672	0.929	0.424	0.889
10th	0.633	0.067	0.192	0.502	0.763	1.001	0.494	0.889
25th	0.693	0.060	0.058	0.575	0.811	1.089	0.553	0.889
50th	0.708	0.063	**0.040**	0.585	0.832	1.219	0.588	0.778
75th	0.715	0.065	**0.035**	0.588	0.842	1.445	0.565	0.889
90th	0.727	0.071	**0.026**	0.588	0.865	1.611	0.541	0.889
95th	0.738	0.071	**0.019**	0.598	0.878	1.594	0.576	0.778

The test result variable(s): Kurtosis, p75, p95 has at least one tie between the positive actual state group and the negative actual state group.
[a] Under the nonparametric assumption
[b] Null hypothesis: true area =0.5
ROC: Receiver operating characteristic, ADC: Apparent diffusion coefficient, AUC: Area under the curve

to Li et al. (9), the whole tumor quantitative ADC histogram may be useful in differentiating between MFAML and RCC. According to the findings of our research, the ADCmin, ADCmedian, ADCmean, ADCmax, 5th, 10th, 25th, 50th, 75th, 90th, and 95th percentiles were all lower for the AML group than they were for the RCC group. This finding is consistent with the findings of other studies published in the literature. A statistically significant difference was found between the ADCmax value ($p<0.001$) and the ADCmedian value, as well as the 50th, 75th, 90th, and 95th percentiles of the ADC values ($p<0.05$). It was hypothesized that the more limited water molecule transport in MFAML caused the lower ADC, and this hypothesis was in line with the findings of other investigations. One explanation is that the presence of adipose tissue and smooth muscle cells restricts the transport of water molecules (14). Since the adipose tissue contains very little water, even a small percentage of fat in MFAML can significantly lower the ADC value.

The asymmetry of the histogram is referred to as skewness (16,17). ADC texture analysis of ccRCC can provide a noninvasive method for accurately detecting high-staged tumors on preoperative imaging, as found by Kierans et al. (18), who found that ccRCC where in skewness based on ADC maps was much greater in high-staged tumors than in low-staged tumors. Our research showed that MFAML had much higher skewness than ccRCC. It showed that most MFAML ADC values were clustered to the left of the histogram in the low ADC values region, whereas most ccRCC ADC values were clustered to the right of the histogram in the high ADC values area. Due to the varying proportions of smooth muscle cells, adipose tissue, and tortuous blood arteries, the ADC value distribution was asymmetric and the skewness tended to be positive in MFAML, whereas in ccRCC, the ADC value was more concentrated and probably normal.

In our study, the AUC for distinguishing MFAML from ccRCC was higher with the 75th percentile ADC with the mean ADC. It was suggested that the higher percentile of the ADC value may be more representative for discriminating MFAML and ccRCC than the lower percentiles, which is consistent with a finding that is very similar to this one made by Tanaka et al. (7). This may be explained by the fact that the tiny necrotic components or cystic cavities of the malignant kidney tumor raise the ADC levels. As a result, the ADC value in the upper percentile may have better sensitivity and specificity.

Our research included several limitations and strengths. First, a limited number of people participated in the research. Second, because this was a retrospective study, there were naturally occurring biases in the selection of patients. Our use of whole-tumor ROI, which boasts superior reproducibility to single-slice ROI, was one of the key factors that contributed to the success of our research.

CONCLUSION

Our research showed that a whole tumor histogram and textural analysis of ADC values could be useful in distinguishing MFAML from RCC. It can increase the diagnostic accuracy and contribute to the process of determining an effective treatment approach.

ETHICS

Ethics Committee Approval: An approval from an University of Health Sciences Türkiye, Bakırköy Dr. Sadi Konuk Training and Research Hospital Clinical Research Ethics Committee was obtained for the study (decision no: 2023-01-15, date: 09.01.2023).

Informed Consent: Retrospective study.

Authorship Contributions

Concept: Ö.A., E.İ., Design: Ö.A., E.İ., Data Collection or Processing: Ö.A., F.T., M.O.N., Analysis or Interpretation: Ö.A., F.T., M.O.N., E.İ., Literature Search: Ö.A., F.T., M.O.N., Writing: Ö.A.

Conflict of Interest: No conflict of interest was declared by the authors.

Financial Disclosure: The authors declare that this study received no financial support.

REFERENCES

1. Katabathina VS, Vikram R, Nagar AM, Tamboli P, Menias CO, Prasad SR. Mesenchymal neoplasms of the kidney in adults: imaging spectrum with radiologic-pathologic correlation. Radiographics 2010;30:1525-40.
2. Kim JK, Park SY, Shon JH, Cho KS. Angiomyolipoma with minimal fat: differentiation from renal cell carcinoma at biphasic helical CT. Radiology 2004;230:677-84.
3. Kim JK, Kim SH, Jang YJ, Ahn H, Kim CS, Park H, et al. Renal angiomyolipoma with minimal fat: differentiation from other neoplasms at double-echo chemical shift FLASH MR imaging. Radiology 2006;239:174-80.
4. Li H, Liang L, Li A, Hu Y, Hu D, Li Z, et al. Monoexponential, biexponential, and stretched exponential diffusion-weighted imaging models: Quantitative biomarkers for differentiating renal clear cell carcinoma and minimal fat angiomyolipoma. J Magn Reson Imaging 2017;46:240-7.
5. Wang H, Cheng L, Zhang X, Wang D, Guo A, Gao Y, et al. Renal cell carcinoma: diffusion-weighted MR imaging for subtype differentiation at 3.0 T. Radiology 2010;257:135-43.
6. Yu X, Lin M, Ouyang H, Zhou C, Zhang H. Application of ADC measurement in characterization of renal cell carcinomas with different pathological types and grades by 3.0T diffusion-weighted MRI. Eur J Radiol 2012;81:3061-6.

7. Tanaka H, Yoshida S, Fujii Y, Ishii C, Tanaka H, Koga F, et al. Diffusion-weighted magnetic resonance imaging in the differentiation of angiomyolipoma with minimal fat from clear cell renal cell carcinoma. Int J Urol 2011;18:727-30.
8. Hötker AM, Mazaheri Y, Wibmer A, Zheng J, Moskowitz CS, Tickoo SK, et al. Use of DWI in the Differentiation of Renal Cortical Tumors. AJR Am J Roentgenol 2016;206:100-5.
9. Li H, Li A, Zhu H, Hu Y, Li J, Xia L, et al. Whole-Tumor Quantitative Apparent Diffusion Coefficient Histogram and Texture Analysis to Differentiation of Minimal Fat Angiomyolipoma from Clear Cell Renal Cell Carcinoma. Acad Radiol 2019;26:632-9.
10. Chen LS, Zhu ZQ, Wang ZT, Li J, Liang LF, Jin JY, et al. Chemical shift magnetic resonance imaging for distinguishing minimal-fat renal angiomyolipoma from renal cell carcinoma: a meta-analysis. Eur Radiol 2018;28:1854-61.
11. Just N. Improving tumour heterogeneity MRI assessment with histograms. Br J Cancer 2014;111:2205-13.
12. Li XL, Shi LX, Du QC, Wang W, Shao LW, Wang YW. Magnetic resonance imaging features of minimal-fat angiomyolipoma and causes of preoperative misdiagnosis. World J Clin Cases 2020;8:2502-9.
13. Chen CL, Tang SH, Wu ST, Meng E, Tsao CW, Sun GH, et al. Calcified, minimally fat-contained angiomyolipoma clinically indistinguishable from a renal cell carcinoma. BMC Nephrol 2013;14:160.
14. Hindman N, Ngo L, Genega EM, Melamed J, Wei J, Braza JM, et al. Angiomyolipoma with minimal fat: can it be differentiated from clear cell renal cell carcinoma by using standard MR techniques? Radiology 2012;265:468-77.
15. Tordjman M, Mali R, Madelin G, Prabhu V, Kang SK. Diagnostic test accuracy of ADC values for identification of clear cell renal cell carcinoma: systematic review and meta-analysis. Eur Radiol 2020;30:4023-38.
16. Zhang Y, Chen J, Liu S, Shi H, Guan W, Ji C, et al. Assessment of histological differentiation in gastric cancers using whole-volume histogram analysis of apparent diffusion coefficient maps. J Magn Reson Imaging 2017;45:440-9.
17. Baek HJ, Kim HS, Kim N, Choi YJ, Kim YJ. Percent change of perfusion skewness and kurtosis: a potential imaging biomarker for early treatment response in patients with newly diagnosed glioblastomas. Radiology 2012;264:834-43.
18. Kierans AS, Rusinek H, Lee A, Shaikh MB, Triolo M, Huang WC, et al. Textural differences in apparent diffusion coefficient between low- and high-stage clear cell renal cell carcinoma. AJR Am J Roentgenol 2014;203:W637-44.